Biosensors and Bioelectronics 58 (2014) 237–241

Contents lists available at ScienceDirect

Biosensors and Bioelectronics

journal homepage: www.elsevier.com/locate/bios

Ultrasensitive dopamine sensor based on novel molecularly imprinted polypyrrole coated carbon nanotubes

Tao Qian [a], Chenfei Yu [a], Xi Zhou [a], Peipei Ma [a], Shishan Wu [a,*], Lina Xu [a], Jian Shen [a,b,**]

[a] School of Chemistry and Chemical Engineering, Nanjing University, Nanjing 210093, China
[b] Jiangsu Collaborative Innovation Center of Biomedical Functional Materials, Nanjing 210046, China

ARTICLE INFO

Article history:
Received 9 January 2014
Received in revised form
27 February 2014
Accepted 28 February 2014
Available online 12 March 2014

Keywords:
Polypyrrole
Carbon nanotubes
Molecularly imprinted polymers
Dopamine
Electrochemical sensor

ABSTRACT

A novel electrochemical sensor using the molecularly imprinted (MIP) oxygen-containing polypyrrole (PPy) decorated carbon nanotubes (CNTs) composite was proposed for in vivo detection of dopamine (DA). The prepared sensor exhibits a remarkable sensitivity of (16.18 μA/μM) with a linear range of 5.0×10^{-11}–5.0×10^{-6} M and limit of detection as low as 1.0×10^{-11} M in the detection of DA, which might be due to the plenty cavities for binding DA through π–π stacking between aromatic rings and hydrogen bonds between amino groups of DA and oxygen-containing groups of the novel PPy.

1. Introduction

Dopamine (DA) is a catecholamine neurotransmitter of significant biologic interest, for its demonstration of the treatment of the central nervous system disorders, such as schizophrenia and Parkinson's disease (Hyman and Malenka, 2001). Hence, an accurate and sensitive determination of DA is vitally important in the diagnostics of various mental diseases. While the determination remains a challenge because of its coexistence with other high concentrations biomolecules in biological samples. To solve the problem, a variety of strategies (Yu et al., 2012; Xu and Yoon, 2011; Song et al., 2012; Lee et al., 2012; Qian et al., 2013b) have been used to detect DA since the 1970s. However, many of these methods do not meet the growing requirements for developing more selective and sensitive sensors for DA. Therefore, the further development of simple, cost-effective methods with high sensitivity and selectivity for detecting DA is highly desirable.

Carbon nanomaterials have attracted a great deal of attention in different research fields for their fascinating chemical, electronic and mechanical properties (Ju et al., 2009). Among them, carbon nanotubes (CNTs) have been widely utilized in the detection of biomolecules, owing to their unique structures, high stabilities, low resistivities, and high surface-to-volume ratios (Heller et al., 2005; Kumar et al., 2010).

Molecular imprinting technique is a system of design and construction of materials with specific receptor sites for a high attraction to the target molecule. Because of obvious advantages such as thermal stability, physical robustness, low cost and easy preparation, molecular imprinting polymers (MIPs) have been proved as a promising method for biomolecules recognition (Baggiani et al., 2012). Recently, many routes have been explored to develop surface MIPs composites for detection of DA, Gu et al. (2013) reported a competitive sensor for the specific capture of dopamine using boronic acid functional groups based on molecularly imprinted technique, Zeng et al. (2013) prepared a composite of SiO_2-coated Graphene Oxide MIPs for dopamine detection. With regard to the selection of the polymer materials, polypyrrole (PPy) is a suitable candidate for in vivo recording of DA because of its ease of fabrication, high conductivity, and good biocompatibility (Qian et al., 2013c; Su et al., 2012; Fabregat et al., 2011). Besides, the presence of an amine group on the pyrrole ring may lead to enhancement of biomolecular sensing (Qian et al., 2013a). In this study, a novel kind of PPy has been fabricated through in situ chemical oxidative polymerization on the surface of CNTs in the presence of DA (Fig. 1). Such polymerization may result in oxygen-containing groups being incorporated into the PPy backbone, which may attract the electropositive groups of DA and also repel anionic molecules such as ascorbic acid (AA) (Tsaia et al., 2012). The prepared PPy/CNTs-MIPs exhibit admirable sensitivity and selectivity in the electrochemical detection of DA in real samples.

* Corresponding author. Tel./fax: +86 83316661.
** Corresponding author at: School of Chemistry and Chemical Engineering, Nanjing University, Nanjing 210093, China. Tel./fax: +86 83316661.
E-mail addresses: shishanwu@nju.edu.cn (S. Wu), shenj57@nju.edu.cn (J. Shen).

http://dx.doi.org/10.1016/j.bios.2014.02.081
0956-5663/

2. Materials and methods

2.1. Reagents and chemicals

Pyrrole (AR) and hydrogen peroxide (H_2O_2, 30% AR) were purchased from Sinopharm Chemical Reagent Co. (China). $FeCl_2$ (AR) was purchased from Shanghai Chemical Reagent Co. (China). Multi-walled carbon nanotubes (CNTs, purity $>95\%$, diameter 40–60 nm, length $<2\ \mu m$) were purchased from Shenzhen Nanotech Port Co. Ltd. (China). Deionized water was applied for all polymerization and reaction processes. AA, DA and uric acid (UA) were purchased from Aladdin Chemical Reagent Co. (China). Human serum and urine were provided by the local hospital and stored at 4 °C.

2.2. Apparatus

Transmission electron microscopy (TEM) images were obtained with a JEM 2100 high-resolution TEM. Raman analysis was performed with a Jobin Yvon HR800. X-ray photoelectron spectroscopy (XPS) measurements were performed on a PHI 5000 VersaProbe. UV–vis spectra were obtained with a Lambda 35 UV–vis

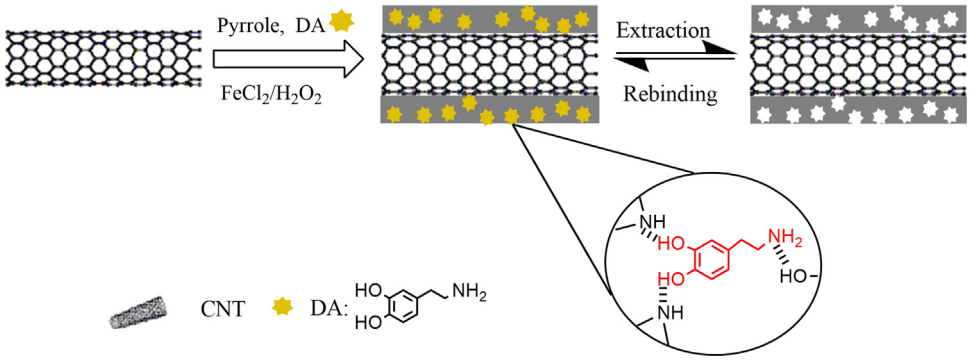

Fig. 1. The chemical route to the preparation of PPy/CNTs-MIPs.

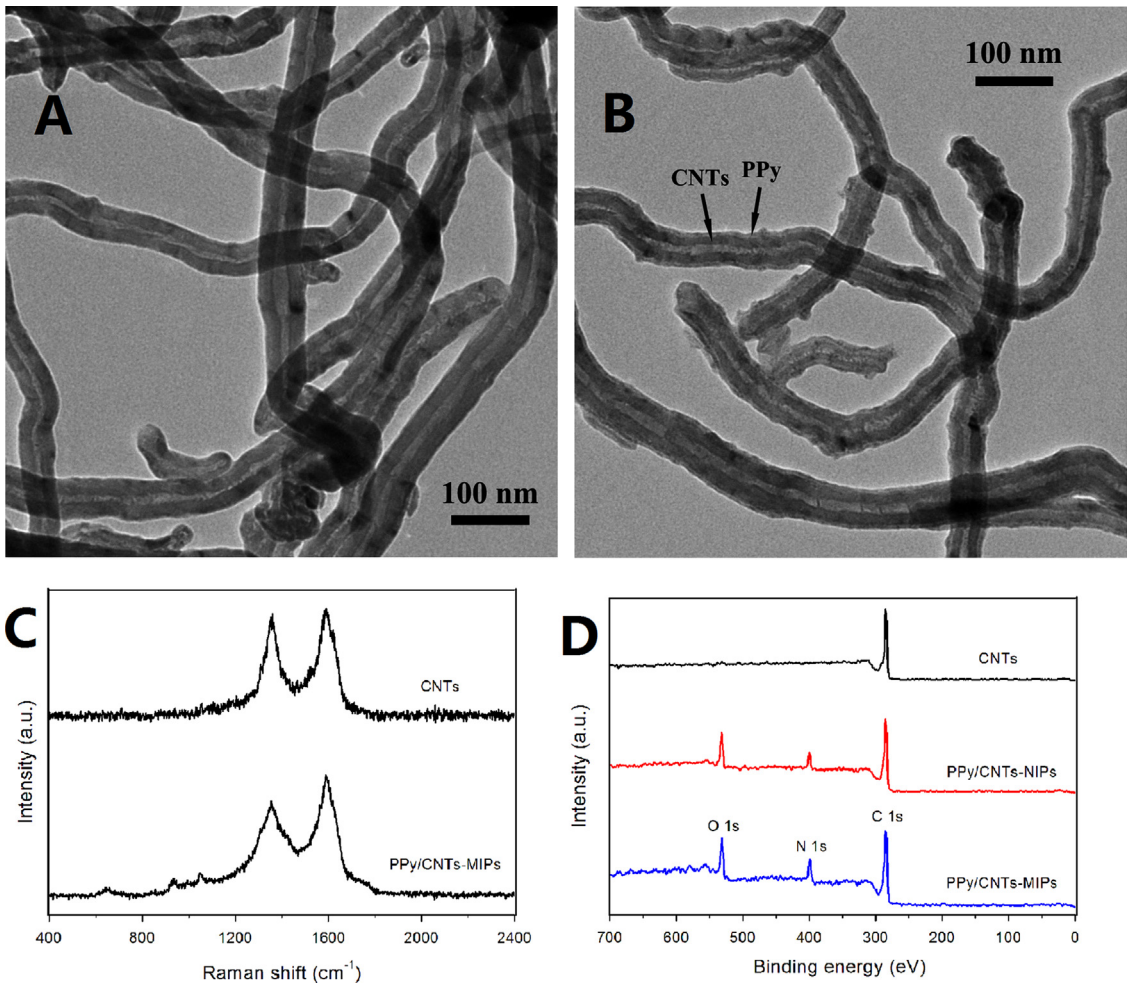

Fig. 2. TEM images of (A) CNTs, and (B) PPy/CNTs-MIPs; (C) Raman spectra of CNTs and PPy/CNTs-MIPs; (D) XPS spectra of the pristine CNTs, prepared PPy/CNTs-NIPs and PPy/CNTs-MIPs composites.

spectrometer. All electrochemical measurements were carried out with a CHI660D (Shanghai CH Instrument Company, China). Cyclic voltammetry (CV) and differential pulse voltammetry (DPV) were performed with a conventional three-electrode system consisting of a bare or modified glassy carbon electrode (GCE; diameter=3 mm) as the working electrode, a saturated calomel electrode (SCE) as the reference electrode, and a platinum wire as the counter electrode.

2.3. Fabrications of the PPy/CNTs-MIPs and PPy/CNTs-NIPs sensors

PPy/CNTs-MIPs were initiated with the addition of 0.5 mL H_2O_2 to the CNTs/pyrrole/$FeCl_2$/DA/H_2O (0.1 g/0.1 mL/0.01 g/0.1 g/100 mL) mixture and lasted for 6 h. After that, the hybrid was washed with water to remove the dopamine. Subsequently, composite dispersion (0.1 wt%) was dropped on the surface of GCE and dried by infrared lamp. The embedded DA were further extracted by scanning between −0.2 and +0.7 V in 0.5 M KOH and in 0.1 M phosphate buffer solution (PBS, pH 6.5) for several cycles until no obvious oxidation peak for DA could be observed, the sensor was stored under 4 °C when not in use. Preparation processes of PPy/CNTs-NIPs sensors were as same as the method mentioned above but without the addition of DA.

3. Results and discussion

3.1. Structure and morphology

To investigate the morphology of the fabricated PPy/CNTs-MIPs composite, TEM images were carried out and results were shown in Fig. 2A and B. The image of pure CNTs shows a typically smooth surface in Fig. 2A. By contrast, the surface of nanotubes is rougher after the decoration of PPy (Fig. 2B), and the diameter increase with the addition of PPy particles, which also illustrates a successful decoration of PPy shell on the CNTs. The decorative PPy shell could prevent the aggregation of pristine CNTs and lead to a high dispersibility. Fig. S1 displays the photos of the dispersions after sonication to reveal the dispersibility directly. It can be seen that the resulting dispersion of fabricated composites remain well-dispersed in water for at least 24 h. But we are unable to prepare stable CNTs suspensions without the decoration of PPy. The result was further confirmed by UV–vis spectroscopy. Individual CNTs is active in the UV–vis region and exhibit characteristic bands (Kataura et al., 1999), however, bundled CNTs is hardly active in the wavelength region between 200 and 600 nm most probably because of carrier are tunneling (Fig. S2a) (Laurent et al., 2003). The increasing amount of dispersed CNTs results in an increasing absorbance of the spectrum. The UV–vis spectra of prepared composite dispersions show a maximum between 200 and 300 nm (Fig. S2c) (Grossiord et al., 2005). All the above phenomena reveal that the PPy particles have successfully coated on the surface of CNTs and leaded a high dispersibility.

The structures of the composites were investigated by Raman spectra as shown in Fig. 2C. The initial CNTs sample represents the typical peaks located at 1355 cm^{-1} and 1590 cm^{-1}, corresponding to the disorder mode (D-band) and tangential mode (G-band), respectively. The D/G band intensity ratio expresses the atomic ratio of sp^3/sp^2 carbons, which is a measure of the extent of disordered graphite (Eda and Chhowalla, 2010). The I_D/I_G changes from 0.96 for the pristine CNTs sample to 0.78 for the one decorated with PPy particles. Meanwhile, the characteristic peak for PPy of C–H out-of-plane deformation, ring deformation and C–H inplane deformation at 925, 981, and 1039 cm^{-1} could be observed in the spectrum of composite. Both of these phenomena also imply the successful fabrication of PPy/CNTs-MIPs hybrids.

XPS is a powerful technique to discern the surface chemical species of materials. Therefore, the synthesized hybrid materials have been subject to XPS analysis (Fig. 2D). The peaks of N 1s and O 1s in the prepared composites are obviously observed compare with the pristine CNTs, which further confirm that PPy with oxygen-containing groups has successfully decorated on CNTs. Moreover, XPS analysis of DA-imprinted hybrid exhibits that signals in N 1s and O 1s are substantially raised in comparison with those of NIPs.

3.2. Template extraction and adsorption of PPy/CNTs-MIPs

The conventional method for template extraction is using organic reagents or buffer solution as eluent. However, it is time consuming and the template cannot be removed entirely. In this work, a simple method, cyclic voltammetry, was presented to extract DA molecules from the imprinted material until there was no obvious signal of DA. After about 20 cycles scanning of CV in 0.5 M KOH, the current response was kept stable to nearly zero (Fig. S3), which demonstrated the complete removal of template molecules.

The adsorption kinetics of DA was investigated by varying the adsorption time from 30 s to 10 min, and the initial concentration of DA kept constant at 1.0×10^{-6} M (Fig. S4). The peak current increased rapidly with the incubation time from 0 to 2 min and then leveled off after 2 min. The result reveals rapid response equilibrium of DA molecules to PPy/CNTs-MIPs, which might be due to the surface binding sites of PPy/CNTs-MIPs composite through π−π stacking between aromatic rings and hydrogen bonds between amino groups of DA and oxygen-containing groups of the novel PPy.

3.3. Electrochemical properties

The advantages of the PPy/CNTs-MIPs were firstly demonstrated by CV (Fig. 3). The comparison shows that the characteristic oxidation peak of DA at the PPy/CNTs-NIPs (curve b) modified GCE is higher than that at the pristine CNTs (curve a) modified one. In addition, the baseline obtained at the former was greatly enhanced as compared to the latter, which mostly because of the decoration of PPy particles, and prevented the aggregation of CNTs. The current response of PPy/CNTs-MIPs (curve c) modified GCE was nearly 5.4 times that of PPy/CNTs-NIPs. The phenomenon could be explained that the MIPs have plenty cavities for binding DA.

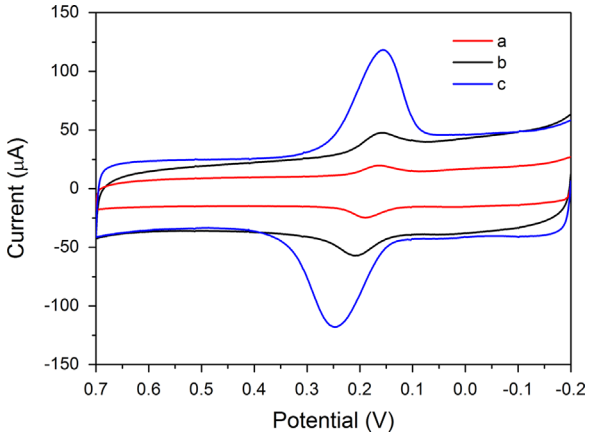

Fig. 3. CVs of the (a) PPy/CNTs-MIPs (b) PPy/CNTs-NIPs, and (c) CNTs doped GCE in 0.1 M PBS (pH 6.5) in the presence of DA (1.0×10^{-5} M) at a scan rate of 100 mV s^{-1}.

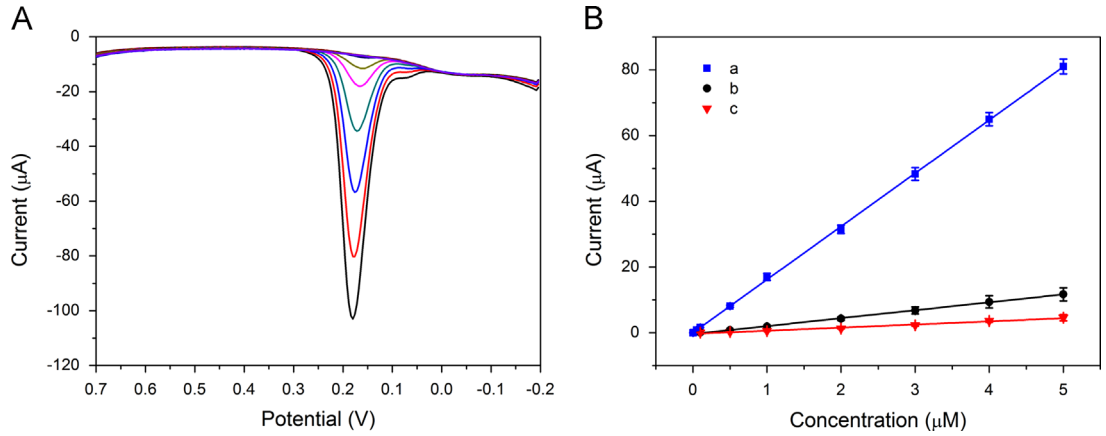

Fig. 4. (A) The DPVs of increasing DA concentration in 0.1 M PBS (pH 6.5), DA concentration was 5.0×10^{-11}, 1.0×10^{-10}, 5×10^{-10}, 1.0×10^{-9}, 5.0×10^{-9}, 1.0×10^{-8}, 5.0×10^{-8}, 1.0×10^{-7}, 5.0×10^{-7}, 1.0×10^{-6}, 2.0×10^{-6}, 3.0×10^{-6}, 4.0×10^{-6}, and 5.0×10^{-6} M (from top to bottom), respectively (D) The calibration curve of DA obtained with (a) PPy/CNTs-MIPs (RSD < 3.0%), (b) PPy/CNTs-NIPs (RSD < 3.0%), and (c) CNTs modified GCE (RSD < 3.0%).

Table 1
Comparison of the proposed PPy/CNTs-MIPs modified electrode with other electrochemistry methods in the determination of DA.

Modified materials	Detection limit (M)	Linear range (M)	Sensitivity (μA/μM)	Method	References
MIPs/MWNTs[a]	6.0×10^{-8}	6.25×10^{-7}–1.0×10^{-4}	0.086	DPV	Kan et al. (2012)
AuNPs@SiO_2-MIP[b]	2.0×10^{-8}	4.8×10^{-8}–5.0×10^{-5}	0.0417	DPV	Yu et al. (2012)
GO/SiO_2-MIPs[c]	3.0×10^{-8}	5.0×10^{-8}–1.6×10^{-4}	0.0047	Amperometry	Zeng et al. (2013)
AuNPs@MIPs[d]	7.8×10^{-9}	2.0×10^{-8}–5.6×10^{-7}	0.2443	Amperometry	Xue et al. (2013)
GSCR-MIPs[e]	1.0×10^{-7}	1.0×10^{-7}–8.3×10^{-4}	0.025	Amperometry	Mao et al. (2011)
PPy/CNTs-MIPs	1.0×10^{-11}	5.0×10^{-11}–5.0×10^{-6}	16.18	DPV	This work

[a] Molecularly imprinted polypyrrole-multiwalled carbon nanotubes.
[b] Gold nanoparticles and SiO_2 molecularly imprinted polymers.
[c] SiO_2-coated graphene oxide and molecularly imprinted polymers.
[d] Gold nanoparticles doped molecularly imprinted polymers.
[e] Graphene sheets/Congo red-molecular imprinted polymers.

Fig. 4A displays the DPV responses of the PPy/CNTs-MIPs modified electrode after incubation in the DA solution. The sharp and well-defined oxidation peak current increased with template molecule concentration. A good linear region with a concentration of DA in the range 5.0×10^{-11}–5.0×10^{-6} M is shown in Fig. 4B, line a. The linear regression equation was expressed as I_{pa} (μA)= 0.0144+16.18C_{DA} (μM) with a correlation coefficient of R^2= 0.9998. The detection limit is 1.0×10^{-11} M based on the signal corresponding to three times the noise of the response (Fig. S6). The slope of the calibration plot for DA at prepared composite is 16.18, which is much higher compared to those obtained by PPy/CNTs-NIPs (slope: 2.41, R^2=0.9991, Fig. 4B, line b) and CNTs (slope: 0.94, R^2=0.9986, Fig. 4B, line c). As shown in Table S1, the results of PPy/CNTs-MIPs sensor for detecting DA are compared with that of other published electrochemical methods (Table 1), which demonstrated high sensitivity and low detection limit of the prepared PPy/CNTs-MIPs sensor, indicating the advantages of such hybrid.

Generally, coexisting electroactive components such as AA and UA show serious interference in the electrochemical detection of DA. Fig. S7 shows DPVs of the PPy/CNTs-MIPs modified electrode for 5×10^{-6} M DA, in the presence of 1.25×10^{-4} M AA and 3.3×10^{-4} M UA. It can be seen that the oxidation peaks of AA, DA and UA appear at potentials of −0.076 V, 0.184 V and 0.336 V, respectively, and the sensor is more sensitive towards DA. The separation of the oxidation peak potentials for UA-DA, DA-AA and UA-AA is about 152 mV, 260 mV and 412 mV, respectively, which allow selective determination of DA in the presence of the other two species.

To evaluate the applicability of the proposed sensor, the concentration of DA in human serum and urine samples were determined applying the standard addition method. The analytical results are shown in Table 2 and Fig. S8. The recovery is in the range of 97.20–103.30%, indicating that the sensor has good accuracy and great potential for practical application for the analysis of DA in real samples.

To investigate the reproducibility of the proposed method, five parallel measurements of 5.0×10^{-6} M DA were carried out. The relative standard deviation (RSD) is 2.13%, indicating that the PPy/CNTs-MIPs modified electrode has good reproducibility. The storage stability of the proposed sensor was also examined by monitoring the current response at 5.0×10^{-6} M DA. When not in use, the sensor was stored at 4 °C. It is found that the DPV current response of lost only 4.65% of the initial response after one month in our work, demonstrating that the PPy/CNTs-MIPs modified electrode possess good stability.

4. Conclusion

In conclusion, PPy/CNTs-MIPs have been fabricated via a facile process. The unique PPy with plenty cavities could binding DA through π–π stacking between aromatic rings and hydrogen bonds between amino groups of DA and oxygen-containing groups of the polymer. Such novel electrochemical sensor exhibits superiority as high current response, low detection limit and good selectivity, indicating the advantages of PPy/CNTs-MIPs composite. Moreover, the accurate analysis in real samples provides a promising

Table 2
Determinations of DA in human serum and urine samples.

Sample	Added (M)	Found (M)	Recovery (%)	RSD[a] (%)
Serum	5.0×10^{-7}	4.87×10^{-7}	97.40	1.22
	1.0×10^{-6}	1.033×10^{-6}	103.30	2.13
	1.5×10^{-6}	1.532×10^{-6}	102.13	1.35
	2.0×10^{-6}	2.065×10^{-6}	103.25	1.57
	2.5×10^{-6}	2.561×10^{-6}	102.44	0.83
Urine	5.0×10^{-7}	5.12×10^{-7}	102.40	1.45
	1.0×10^{-6}	0.972×10^{-6}	97.20	1.63
	1.5×10^{-6}	1.471×10^{-6}	98.07	0.94
	2.0×10^{-6}	2.041×10^{-6}	102.05	1.84
	2.5×10^{-6}	2.432×10^{-6}	97.28	1.62

[a] RSD value reported is for $n=3$. The serum and urine samples were diluted 100 times with PBS (pH=6.5) before measurement. No other pretreatment process was performed.

potential utility in the clinical settings for the diagnosis of DA-related diseases.

Acknowledgments

This work was supported by the National Natural Science Foundation of China (Nos. 51272100 and 51273073) and the Foundation of Jiangsu Collaborative Innovation Center of Biomedical Functional Materials.

Appendix A. Supporting information

Supplementary data associated with this article can be found in the online version at http://dx.doi.org/10.1016/j.bios.2014.02.081.

References

Baggiani, C., Giovannoli, C., Anfossi, L., Passini, C., Baravalle, P., Giraudi, G., 2012. J. Am. Chem. Soc. 134, 1513–1518.
Eda, G., Chhowalla, M., 2010. Adv. Mater. 22, 2392–2415.
Fabregat, G., Córdova-Mateo, E., Armelin, E., Bertran, O., Alemán, C., 2011. J. Phys. Chem. C 115, 14933–14941.
Grossiord, N., Regev, O., Loos, J., Meuldijk, J., Koning, C.E., 2005. Anal. Chem. 77, 5135–5139.
Gu, L., Jiang, X.Y., Liang, Y., Zhou, T.S., Shi, G.Y., 2013. Analyst 138, 5461–5469.
Heller, D.A., Baik, S., Eurell, T.E., Strano, M.S., 2005. Adv. Mater. 17, 2793–2799.
Hyman, S.E., Malenka, R.C., 2001. Nat. Rev. Neurosci. 2, 695–703.
Ju, S.Y., Kopcha, W.P., Papadimitrakopoulos, F., 2009. Science 323, 1319–1323.
Kan, X.W., Zhou, H., Li, C., Zhu, A.H., Xing, Z.L., Zhao, Z., 2012. Electrochim. Acta 63, 69–75.
Kataura, H., Kumazawa, Y., Maniwa, Y., Umezu, I., Suzuki, S., Ohtsuka, Y., Achiba, Y., 1999. Synth. Met. 103, 2555–2558.
Kumar, S.A., Wang, S.F., Yang, T.C.K., Yeh, C.T., 2010. Biosens. Bioelectron. 25, 2592–2597.
Laurent, J.S., Voisin, C., Cassabois, G., Delalande, C., Roussignol, P., Jost, O., Capes, L., 2003. Phys. Rev. Lett. 90057404-1–057404-4
Lee, H.C., Chen, T.H., Tseng, W.L., Lin, C.H., 2012. Analyst 137, 5352–5357.
Mao, Y., Bao, Y., Gan, S.Y., Li, F.H., Niu, L., 2011. Biosens. Bioelectron. 28, 291–297.
Qian, T., Wu, S.S., Shen, J., 2013a. Chem. Commun. 49, 4610–4612.
Qian, T., Yu, C.F., Wu, S.S., Shen, J., 2013b. Biosens. Bioelectron. 50, 157–160.
Qian, T., Yu, C.F., Wu, S.S., Shen, J., 2013c. J. Mater. Chem. A 1, 6539–6542.
Song, P., Mabrouk, O.S., Hershey, N.D., Kennedy, R.T., 2012. Anal. Chem. 84, 412–419.
Su, Z.H., Liu, Y., Xie, Q.J., Chen, L., Zhang, Y., Meng, Y., Li, Y., Fu, Y.C., Ma, M., Yao, S.Z., 2012. Biosens. Bioelectron. 36, 154–160.
Tsaia, T.C., Han, H.Z., Cheng, C.C., Chen, L.C., Chang, H.C., Chen., J.J., 2012. Sens. Actuators B—Chem. 171-172, 93–101.
Xu, Q.L., Yoon, J.Y., 2011. Chem. Commun. 47, 12497–12499.
Xue, C., Han, Q., Wang, Y., Wu, J.H., Wen, T.T., Wang, R.Y., Hong, J.L., Zhou, X.M., Jiang, H.J., 2013. Biosens. Bioelectron. 49, 199–203.
Yu, D.J., Zeng, Y.B., Qi, Y.X., Zhou, T.S., Shi, G.Y., 2012. Biosens. Bioelectron. 38, 270–277.
Zeng, Y.B., Zhou, Y., Kong, L., Zhou, T.S., Shi, G.Y., 2013. Biosens. Bioelectron. 45, 25–33.